*Cerebral Cortex*, January 2018;28: 167–183

**doi: 10.1093/cercor/bhw365**
Advance Access Publication Date: 5 December 2016
Original Article

ORIGINAL ARTICLE

# Functional Characterization of the Left Ventrolateral Premotor Cortex in Humans: A Direct Electrophysiological Approach

L. Fornia[1], V. Ferpozzi[1], M. Montagna[2], M. Rossi[3], M. Riva[4], F. Pessina[4], F. Martinelli Boneschi[5], P. Borroni[6], R. N. Lemon[7], L. Bello[3], and G. Cerri[1]

[1]Laboratory of Motor Control, Department of Medical Biotechnologies and Translational Medicine, Università degli Studi di Milano, Humanitas Research Hospital, IRCCS, Milano, 20089, Italy, [2]Laboratory of Motor Control, Department of Medical Biotechnologies and Translational Medicine, Università degli Studi di Milano, Milano, 20129, Italy, [3]Cancer Neurosurgery Unit, Department of Oncology and Hemato-Oncology, Università degli Studi di Milano, Humanitas Research Hospital, IRCCS, Milano, 20089, Italy, [4]Cancer Neurosurgery Unit, Humanitas Research Hospital, IRCCS, Milano, 20089, Italy, [5]Laboratory of Genetics of Neurological Complex Disorders, Department of Neurology, Institute of Experimental Neurology (INSPE), San Raffaele Scientific Institute and University, Milano, 20132, Italy, [6]Department of Health Sciences, Università degli Studi di Milano, Milano, 20142, Italy and [7]Sobell Department of Motor Neuroscience and Movement Disorders, UCL Institute of Neurology, London, WC1N 3BG, UK

Address correspondence to Gabriella Cerri, Laboratory of Motor Control, Department of Medical Biotechnologies and Translational Medicine, Università degli Studi di Milano, Humanitas Research Hospital, Via Manzoni 56, 20089 Rozzano (Milano), Italy. Email: gabriella.cerri@unimi.it



## Abstract

In monkeys, motor outputs from premotor cortex (PM) involve cortico-cortical connections with primary motor cortex (M1). However, in humans, the functional organization of PM and its relationship with the corticospinal tract (CST) is still uncertain. This study was carried out in 21 patients undergoing intraoperative brain mapping prior to tumor resection. The left ventrolateral premotor cortex (vlPM-BA6) was identified preoperatively by functional magnetic resonance imaging, and then investigated intraoperatively using high frequency direct electrical stimulation (HF-DES) of the convexity of M1 and vlPM-BA6, with simultaneous recording of motor-evoked potentials (MEPs) from oro-facial, hand and arm muscles. The somatotopy, organization of evoked responses, latency of MEPs, and cortical excitability of vlPM-BA6 were compared with reference data from M1. vlPM-BA6 was found to be less excitable, with significantly longer MEP latencies than M1. In addition to the pure oro-facial and hand-arm muscle representation, a "transition oro-hand zone" was identified in vlPM-BA6. The longer latency of vlPM-BA6 MEPs suggests that human vlPM could act on spinal motoneurons either directly through more slowly conducting CST fibers or via less direct pathways through M1, brainstem, or spinal mechanisms. The results help in disclosing the very different roles of vlPM and M1 in motor control.

**Key words:** corticospinal tract, human motor system, MEP, motor control, premotor cortex

## Introduction

Voluntary skilled hand and oro-facial movements, such as those performed during object manipulation and phonoarticulation, are characteristic attributes of the human species. In humans and nonhuman primates, hand and oro-facial motor skills depend critically on the integrity of the frontal motor areas, particularly the primary motor cortex (M1/BA4), the ventrolateral premotor cortex (PM/BA6), and their corticospinal tract (CST) and corticobulbar tract (CBT) projections (Dum and Strick 1991; He et al. 1993, Lemon 2008, 2010).

In the last 2 decades, many studies focused on the ventral sector of the monkey PM, and especially area F5, have demonstrated its crucial role in the control of goal-directed actions performed with the hand (Jeannerod et al. 1995; Umiltà et al. 2008; Bonini et al. 2011; Rizzolatti et al. 2014) and mouth (Ferrari et al. 2003, Coudè et al. 2011) showing a considerable overlap in the representation of the 2 effectors (Maranesi et al. 2012). These studies distinguish vPM from the more dorsal sector of the premotor cortex (dPM), which instead seems to be involved in control of arm movements for reach and grasp (Johnson et al. 1996; Wise et al. 1997; Raos et al. 2004; Hoshi and Tanji 2007).

A functional subdivision of the PM into a ventral and dorsal sector (vPM and dPM) also emerges from human functional magnetic resonance imaging (fMRI) studies: both vPM and dPM are activated by upper limb motor tasks (Binkofski et al. 1999; Ehrsson et al. 2000, 2001; Kantak et al. 2012), while oro-facial motor tasks (including biting and speech-related movements) activate only vPM (Cerri et al. 2015), suggesting that, in analogy with the monkey, this subdivision hosts both hand and oro-facial representations. Penfield and Boldrey (1937), using direct electrical stimulation (DES) of human cerebral cortex, revealed multiple representations of the body in the cortical areas located between the central and precentral sulci, described as Brodmann area BA4 (primary motor cortex) and area BA6aα, closely resembling the somatotopic organization of the monkey's motor cortex. However, since then, no further studies have used this direct approach in humans to investigate the distinguishing features of motor outputs from the primary and premotor cortex.

A recent study, combining intraoperative DES and fMRI paradigms (Cerri et al. 2015), indicated that the human vPM is the analog of the rostral part of nonhuman primate vPM, referred to as area F5 (Gallese et al. 1996), sharing, in both human and nonhuman primates, mirror-like properties coupled with a clear motor output when stimulated. A similar conclusion was reached in a recent human fMRI study (Ferri et al. 2015), based on an action observation paradigm which has been shown, in both fMRI and single neuron studies, to be an effective stimulus for area F5c, in which mirror neurons have been most consistently reported (Orban 2002; Nelissen et al. 2005).

The functional contribution of the corticospinal and corticobulbar projections from premotor cortex PM-BA6 in primates, and particularly in humans, is still being debated. In macaques, although both dPM and vPM contribute some corticospinal projections, they also exert their influence through cortico-cortical projections to M1, which in turn is the major source of the corticospinal tract, with well-established, powerful, and direct actions on spinal motoneurons (Shimazu et al. 2004; Dum and Strick 2005; Lemon 2008). It has been argued that, compared with corticospinal projections from M1, those from vPM play only a minor role in controlling hand movements, mostly terminating in the upper cervical spinal segments and only to a lesser extent directly to the caudal segments of the cervical enlargement, where the motor nuclei innervating the hand muscles are located (Dum and Strick 2002). However, some effects on hand muscle motoneurons may be exerted by vPM indirectly through C3–C4 propriospinal neurons located in the upper cervical cord (Borra et al. 2010; Isa et al. 2013).

Similarly, there are no descending projections from the vPM oro-facial representation to the nucleus ambiguous, suggesting a lack of direct connections with laryngeal motoneurons (Simonyan and Jürgens 2003), and that vPM exerts most of its motor actions on the oro-facial and laryngeal musculature through dense cortico-cortical connections with M1 (Tokuno et al. 1997; Simonyan and Jürgens 2005).

Strong support to this model comes from electrophysiological data obtained by means of intracortical microstimulation (ICMS) and inactivation studies in nonhuman primates, which have shown consistent differences between vPM and M1 hand motor output, probably reflecting the different hierarchical role of these 2 areas in the control of spinal motoneurons. They have suggested that the motor output from vPM in the macaque monkey is mostly mediated through cortico-cortical connections with M1, rather than through the corticospinal projections that arise from vPM itself (Cerri et al. 2003; Shimazu et al. 2004; Schmidlin et al. 2008; Prabhu et al. 2009).

Despite a large number of studies focused on the human vPM, many of its functional aspects remain to be clarified. Among them, the functional connectivity of this area with spinal motoneurons, its somatotopic organization, and its connections with other cortical areas giving rise to the CST and CBT deserve systematic investigation. At present, the best evidence available derives from animal studies and, in humans, is based on investigations with transcranial magnetic stimulation (TMS) or fMRI. In addition, state-of-the-art approaches in human neuroimaging can provide data related to the functional activation of cortical areas and a probabilistic map of the descending or connecting tracts running in the white matter (Bello et al. 2014). These data, though important and relevant, now need to be validated by direct electrophysiological approaches.

Modern intraoperative neurophysiology in the awake (and asleep) patient offers a unique opportunity to investigate the human brain directly. The traditional stimulation protocol adopted in intraoperative brain mapping procedures utilizes a low frequency (LF) stimulation paradigm (Penfield technique 50–60 Hz) (Penfield and Boldrey 1937; Breshears et al. 2015), very different from the stimulation paradigm used to study the functional organization and the motor output from primary and nonprimary motor areas of the nonhuman primate brain (Porter and Lemon 1993). Recently, Bello et al. (2014) implemented a brain mapping technique, which uses high frequency (HF), brief duration stimulation, a paradigm more closely resembling that used in nonhuman primates (Cerri et al. 2003; Raos et al. 2003; Shimazu et al. 2004; Boudrias et al. 2010a, 2010b). This technique, applied to M1 and vPM in the present study, is more effective for mapping the respective motor output, including the onset latency of evoked motor responses. With all due constraints of the clinical setting, data acquired during surgical procedures using this paradigm provide valuable evidence of the organization of the ventrolateral sector of the premotor cortex (vlPM-BA6).

Preliminary data acquired by using this approach have been reported in a previous study combining fMRI and intraoperative neurophysiology (Cerri et al. 2015).

## Materials and Methods

The aim of the study was to investigate, in human patients, the motor output elicited in forearm-hand and oro-facial muscles

by DES of vlPM-BA6 and to compare this output with that elicited by stimulating the primary motor cortex (M1-BA4), providing a measure of functional connectivity with the relevant motoneurons. Motor-evoked potentials (MEPs) elicited in hand and face muscles by DES applied during intraoperative mapping of both cortical areas were recorded, and their main parameters (latency, amplitude, and somatotopic muscle representation) within each area analyzed and compared.

## Patient Selection

In this study, we included 21 patients affected by gliomas, who were candidates for surgery requiring the exposure of the sensory-motor cortex. We only selected patients in whom tumors did not infiltrate and/or reorganize the main areas of interest, that is, the portion of precentral motor areas giving rise to the corticospinal tract, or with tumors involving the neural structures subserving language function at both cortical and subcortical levels. In order to assess all inclusion requirements, each patient underwent an extensive and multidisciplinary preoperative study involving baseline magnetic resonance (MR) studies, fMRI, and diffusion tensor imaging (DTI) with fiber tractography (FT). Volumetric scan analysis was used to define tumor location and volume. Tumor volume was computed on volumetric fluid-attenuated inversion recovery (FLAIR) MRI scans for low-grade gliomas (LGGs) and on postcontrast $T_1$-weighted MRI scans for high-grade gliomas (HGGs). Functional tractography was performed on all patients before the surgery to detect the degree of infiltration of corticospinal and language pathways at both cortical and subcortical levels, and fMRI analysis was conducted to identify possible shifts or disruptions of language and motor functions. This assessment was applied to all patients independently of the location of the tumor (see Fig. 1 for an example).

An additional analysis was performed, which excluded tumor infiltration of the areas of interest and their cortico-cortical and corticospinal projections. Based on a previous study performed in a similar setting (Quiñones-Hinojosa et al. 2003), the minimum distance between posterior border of the tumor and the precentral sulcus was determined using Brainlab software. For all but one of the patients included in the study, the distance between these 2 landmarks was ≥10 mm (mean 19.83 mm; standard deviation [SD] ± 11.9 mm). Only one patient, with a minimum distance of 7.7 mm, was included on the basis that the tissue and the subcortical fibers surrounding the tumor were preserved, as demonstrated by tractography. Morphological and anatomical reconstructions were always carefully checked preoperatively to exclude any significant rearrangement of the premotor–primary motor cortex circuits investigated in this study.

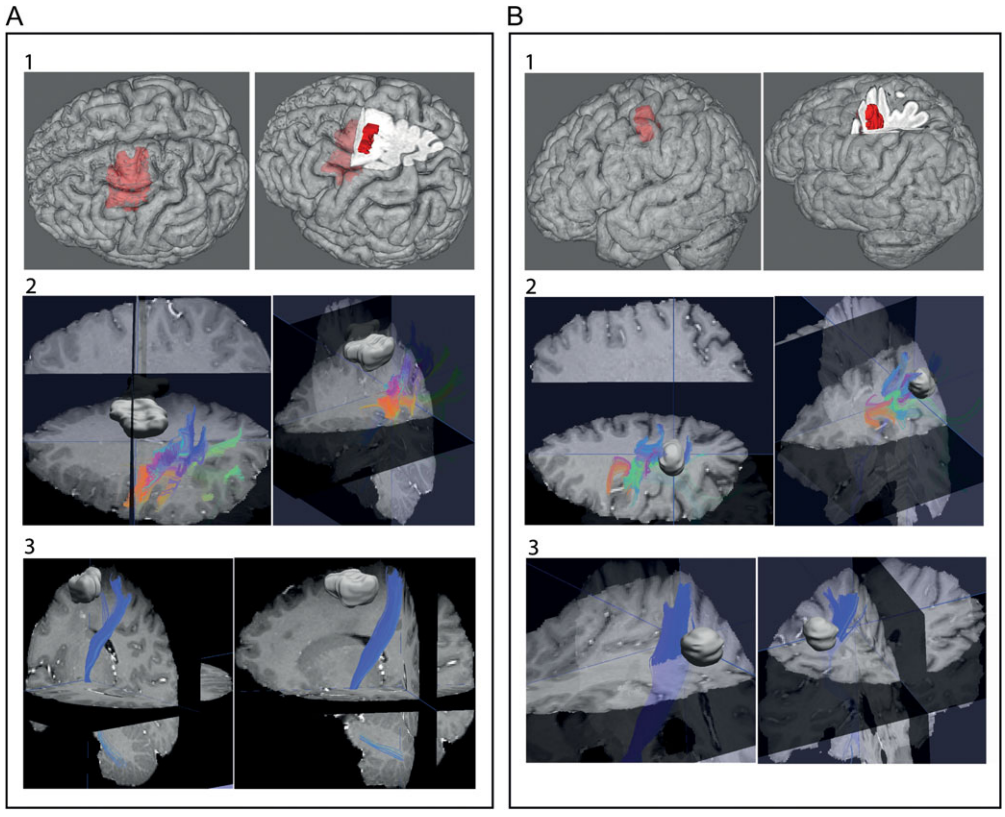


**Figure 1.** (A) Example of a patient included in the study. The tumor was located in the mesial area and did not affect the anatomy of the cortex within the central and precentral sulcus; (B) example of patient excluded from the study. The tumor located across the central sulcus affected the anatomy of the surrounding cortex. For both (A) and (B): panel 1) Anatomical localization of the tumor (in red). Tumor volume was computed on volumetric FLAIR MRI of the patient; in case (A) the posterior margin of the tumor did not reach the precentral sulcus, while in case (B), the tumor was within the central and precentral sulci; panel 2) relationship between fibers within the precentral area and the tumor. DTI reconstruction of the fibers running within the precentral sulcus. The different colors come from combined fractional anisotropy and directional maps. Colors indicates fiber direction as follows: red, left-right; green, antero-posterior; blue, superior-inferior. In case (A), the fibers are not contiguous to the tumor, but this was the case in patient (B). Panel 3) relationship between corticofugal fibers originating from M1 and located close to the tumor. This is based on a DTI reconstruction of the fibers connecting the cerebral peduncles with the M1 forearm-hand area. In case (A) descending fibers are not contiguous to the tumor, it was the case in patient B, displacing adjacent descending fibers.

Histology was classified according to the WHO brain tumor classification. A neurological and neuropsychological evaluation was also performed to exclude neurological and cognitive deficits affecting the motor and/or language function due to the tumor but not detected by the neuroradiological assessment (see Supplementary Table 1 for a detailed clinical description of each patient). Particular attention was given to seizure history and control (number and duration), number and doses of antiepileptic drugs (AEDs), and to the existence of previous treatments (surgery, chemotherapy, or radiotherapy). Thus, we only included patients without sensory-motor and cognitive deficits, cortico-subcortical rearrangement due to tumor infiltration and without seizures, or at least, with a short seizure history that was well controlled by one AED. All patients gave written informed consent to the surgical and mapping procedure, which followed the principles outlined in "World Medical Association Declaration of Helsinki: Research involving human subjects."

The study was performed with strict adherence to the routine procedure normally utilized for surgical tumor removal. Accordingly, all data were recorded utilizing electrophysiological monitoring and stimulating protocols (see below) adopted for routine clinical mapping.

## Presurgical Routine

Preoperatively, all patients were assessed for handedness, neurological examination, and a neuropsychological evaluation of cognitive abilities including nonverbal intelligence, memory, apraxia, and language. The scores obtained by patients enrolled in the study were all within the normal range (see Supplementary Table 1).

Preoperative MR imaging was performed using a Philips Intera 3 T scanner (Best). The neuroradiological examination included basic morphological T1, T2, FLAIR, DWI, and postcontrast T1 images (see Bello et al. 2014 for details). The patients enrolled in the present study were all right handed and were candidates for surgery aimed at removing a tumor located in the left hemisphere. Therefore, the identification of M1 and vlPM-BA6, and the identification of the functional boundaries with the neighboring Brodmann areas 44–45 (Broca's area), was mandatory to determine the surgical safe "cortical point of entry" and to perform the electrophysiological mapping needed to guide surgical tumor removal at the subcortical level. A neuroradiological investigation was therefore performed preoperatively in order to identify the cortical areas and the subcortical tracts essential for voluntary skilled movement (M1 and vlPM-BA6) and language (Broca's area), and to determine the functional and anatomical relationship between these areas/tracts and the tumor. All patients underwent fMRI and DTI-FT. During fMRI, subjects performed a finger tapping task to localize M1, 2 language tasks (covert visual naming and fluency task or covert auditory verb generation) to localize language-related areas, and an action execution-observation grasping task performed with the hand and the mouth to localize vlPM/BA6 (see Cerri et al. 2015). The language hemispheric dominance was determined by the laterality index on the basis of the fMRI results in both language tasks.

Following the fMRI investigation, the DTI-FT technique was used to reconstruct and visualize the fiber tracts running around or inside the tumor, identifying the anatomical boundaries of the lesion. Notably, as a novel method here, the DTI was computed by selecting the cortical region of interests (ROI) based on the areas activated in the fMRI investigation rather than based on the anatomical landmarks. Upon completion of the neuroimaging investigation, the fMRI and the DTI-FT images were loaded into the neuronavigation system for surgical purposes. DTI-FT and FA (fractional Anisotropy) measures excluded the infiltration of the CST–CBT, particularly in the frontal areas neighboring the precentral sulcus and of the language pathways terminating onto the frontal language areas (inferior fronto-occipital and superior longitudinal fasciculi, respectively).

## Surgical Procedure and Routine Intraoperative Protocol

The intraoperative protocol included asleep-awake (-asleep) anesthesia and functional brain mapping by means of electrophysiological and neuropsychological investigation. Total intravenous anesthesia with propofol and remifentanil was used; and no muscle relaxants were employed during surgery to allow mapping of motor responses.

A craniotomy tailored to expose the cortex corresponding to the tumor area and a limited amount of surrounding tissue was performed. In all patients, surgical resection was performed with the aid of the intraoperative neurophysiological brain mapping and monitoring technique (see below). Cortical mapping using DES was performed to define the safe "cortical point of entry," while subcortical brain mapping was performed along with tumor resection, following the principle of locating functional motor or language tracts, which represented in all cases the limit of tumor resection (Bello et al. 2014).

### *Neurophysiological Monitoring*

During surgery, cortical activity was monitored by electroencephalography and electrocorticography (EEG, ECoG, Comet, Grass); ECoG from a cortical region adjacent the area to be stimulated was recorded by subdural strip electrodes (4–8 contacts, monopolar array referred to a midfrontal electrode) throughout the whole procedure, to monitor the basal electrical activity of the brain, and to detect after discharges or electrical seizures during the resection. EEG was recorded with electrodes placed over the scalp in a standard array. EEG and ECoG signals were filtered (bandpass 1–100 Hz), displayed with high sensitivity (50–150 μV/cm and 300–500 μV/cm, respectively) and recorded. The integrity of the descending motor pathways was monitored throughout the procedure using a "train-of-five" pulses delivered to the primary motor (M1) cortex to elicit MEPs, but was suspended during cortical and subcortical mapping to avoid interference. To this aim, a 4-contact subdural strip electrode was placed over the precentral gyrus; each contact was tested, with a vertex reference, by stimulation with trains of 3–5 constant current anodal pulses (pulse duration: 0.5–0.8 ms; interstimulus interval (ISI) within the train: 2–4 ms) at a repetition rate of 1 Hz. The motor threshold (MT) corresponded to the lowest intensity evoking a reproducible MEP (peak-to-peak amplitude >0.02 mV) in at least one distal hand muscle. Electromyographic (EMG) responses to stimulation of the motor areas, as well as the voluntary motor activity, were recorded throughout the procedure by pairs of subdermal hook needle electrodes (Technomed) inserted into 20 muscles (face, upper and lower limb) contralateral to the hemisphere to be stimulated, plus 4 ipsilateral muscles, all connected to a multichannel EMG recording (ISIS-IOM, InomedGmbH) (Bello et al. 2014). Free-running EMG was used to record responses to stimulation and to distinguish between electrical and clinical seizures. Close attention was paid to avoid intraoperative seizures, with continuous monitoring of the ECoG and free-running EMG: at the first ictal sign, stimulation was stopped and cold irrigation of the cortex applied, generally successfully, to abort the seizure.

Whenever the seizures spread to the whole hemibody, a bolus infusion of propofol (4 mL on average) was delivered.

#### *Neurophysiological Brain Mapping*

Two stimulation techniques were routinely used in this procedure: the LF and the HF protocol, according to the frequency of stimulation pulses delivered (Bello et al. 2014). The motor output of M1 and vlPM-BA6 was assessed by analyzing the MEPs elicited with HF stimulation delivered at the cortical level; therefore, the mapping procedure at subcortical level will not be described further (see Bello et al. 2014 for details). The LF paradigm is reported given its crucial role during the procedure for the functional identification, specifically in this sample of patients, of Broca's area and vlPM-BA6 outputs to oro-facial muscles: the disclosure of the boundaries separating these 2 areas is essential for the proper investigation of the vlPM-BA6 with the HF protocol.

The LF stimulation consisted of trains, lasting 1–4 s, of biphasic square wave pulses (0.5 ms each phase) at 60 Hz (ISI 16.6 ms) delivered by a constant current stimulator (OSIRIS-NeuroStimulator) integrated into the ISIS system through a bipolar probe (2 ball tips, 2 mm diameter, separation 5 mm).

HF stimulation was delivered through a monopolar probe (straight tip, 1.5 mm diameter [Inomed], with reference/ground on the skull overlying the central sulcus). HF stimulation was delivered in trains from 1 to 5 constant anodal current pulses (pulse duration 0.5 ms; ISI: 3–4 ms) at variable intensity (1–40 mA) depending on the patient's cortical excitability. HF stimulation is particularly effective in mapping the motor output of nonprimary motor areas such as the premotor cortex (Bello et al. 2014).

The first cortical site to be explored was M1 and the current intensity was initially set at the intensity corresponding to the MT used for MEP monitoring; then the current intensity and the number of pulses were adjusted to the minimum combination effective to evoke reliable MEPs in forearm-hand and/or oro-facial muscles (combined motor threshold, cMT). This protocol was repeated over all the cortical sites of interest, that is, vlPM-BA6, M1, and the adjacent areas (Broca-BA44/45). A given cortical site was considered "not responsive (not eloquent)" when no motor responses could be elicited by increasing the intensity up to a maximum of 40 mA or by increasing the number of pulses up to a maximum of 5.

### Identification of Stimulation Sites on M1 and vlPM-BA6

The anatomo-functional identification of M1 and vlPM-BA6 was established first by preoperative fMRI acquired while patients performed specific tasks (Cerri et al. 2015). fMRI images were loaded into the neuronavigation system. However, neuroimaging data could not fully distinguish Broca's area from vlPM-BA6, or indicate the exact extent of the 2 areas, or the precise boundary between them. During surgery, M1 was identified by applying LF stimulation at the sites previously identified by fMRI data as the centers of the hand and mouth representations. LF stimulation is highly effective when applied over M1, evoking a progressive muscle recruitment and/or tetanic-like muscle response in the resting-state condition. In contrast, when LF stimulation is delivered to vlPM-BA6 at rest, it is less or ineffective in eliciting a motor output. When instead LF stimulation is delivered during a task involving preactivated muscles, it is responsive (Cerri et al. 2015). Therefore, during intraoperative mapping, LF stimulation was applied during performance of language tasks (counting test and naming test) in order to identify and distinguish vlPM-BA6 cortex from the adjacent Broca's area and from M1 (Bello et al. 2006). During these tests, the putative Broca's area indicated on the fMRI images was stimulated with the bipolar probe delivering DES with trains of pulses at 60 Hz (LF: average train duration ± SD: 2.3 ± 0.9 s; average stimulation intensity ± SD: 3.9 ± 0.6 mA). When the stimulation stopped the patient's counting/naming at least 3 times (speech arrest), the localization of Broca's area was considered reliable. During performance of the same tasks, LF stimulation was applied to the most ventral sector of BA6, supposedly vlPM-BA6 as indicated by the fMRI images (LF: average train duration ± SD: 2.1 ± 0.5 s; average stimulation intensity ± SD: 3.6 ± 0.6 mA). When the stimulation induced anarthria (impairment of phono-articulatory muscles active during the task), the identification of the area was considered reliable. Given the demonstrated absence of motor output from Broca's area (Cerri et al. 2015), the vlPM-BA6 cortex was identified as the area from which motor responses could be elicited with HF stimulation.

#### *Motor Output Assessment*

Once vlPM-BA6, M1, and Broca's area (BA44/45) were exposed and functionally identified, the HF protocol was applied to the same cortical loci and surrounding fields to look for the presence of an MEP. In particular, we focused on responses in 6 target muscles contralateral to the left hemisphere, 2 oro-facial muscles, "orbicularis oris" (OO) and "mylohyoid" (MYLO), and 4 forearm-hand muscles, "extensor digitorum communis" (EDC), "abductor pollicis brevis" (APB), "first dorsal interosseous" (FDI), and "abductor digiti minimi" (ADM). HF trains were applied initially to M1 (average stimulation intensity ± SD: 15.4 ± 7.3 mA), over the upper limb and face motor areas in the resting state, with a single shock or a train of pulses depending on the clinical constraints and needs. When a single pulse was applied, the current intensity was adjusted until it evoked a constant response in at least one muscle. When a train of pulses was applied, the intensity was kept constant and number of pulses was progressively increased until it they evoked a constant response in at least one muscle. The maximum number of stimuli applied was 5. The same protocol was applied to vlPM-BA6 (average stimulation intensity ± SD: 20 ± 9.4 mA). During stimulation, the entire set of muscles was recorded simultaneously.

The complex clinical condition and the need to minimize the duration of the clinical procedure meant that a full set of responses in all muscles could not be collected from every patient.

### Data Analysis

#### *Somatotopic Distribution of Motor Responses From M1 and vlPM-BA6*

In 21 patients, we analyzed the distribution of motor responses obtained by DES over "Positive Sites," that is, cortical sites responding to stimulation with an MEP. Stimulation of cortical sites eliciting responses in only one muscle of those recorded (either an oro-facial or a hand-forearm muscle) was denominated "Single Positive Sites"; the cortical sites from which responses in multiple muscles were obtained were defined as "Multiple Positive Sites." Stimulation of a Single Positive Site therefore resulted in oro-facial "or" hand-arm responses, that is, activation of a single muscle in only 1 of the 2 effectors tested. Stimulation of the Multiple Positive Sites resulted in "Simple Muscle Combination Responses" when activating several muscles within the same effector (oro-facial or forearm-hand) and in "Complex Muscle Combinations" when activating several muscles involving both

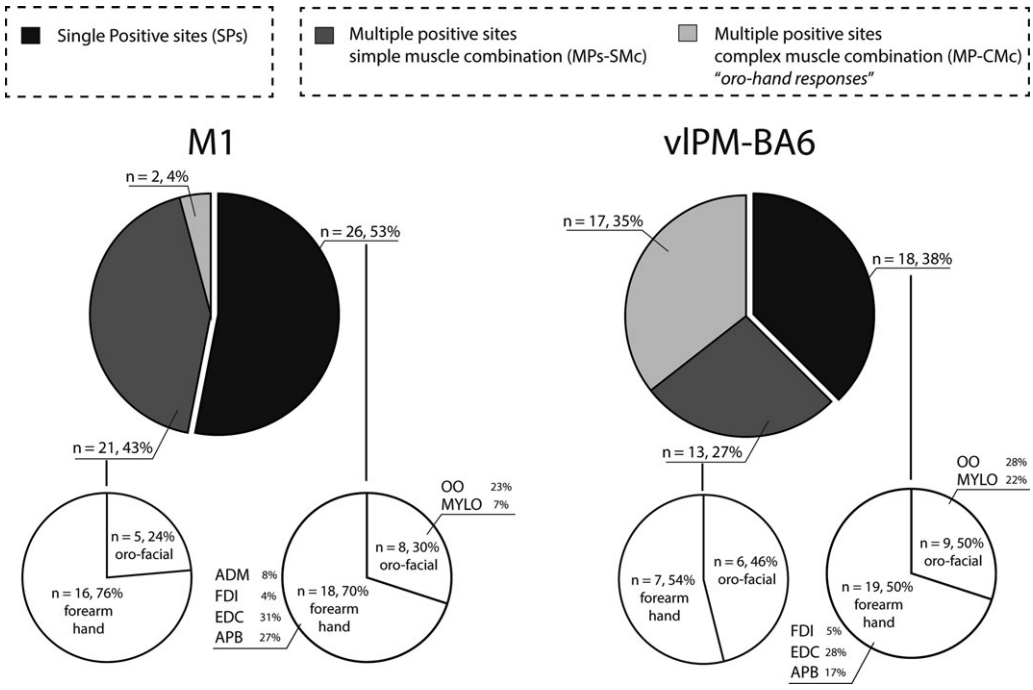


**Figure 2.** Frequency and type of Positive Sites in M1 and vlPM-BA6. We analyzed the distribution of motor responses obtained by DES from "Positive Sites," that is, cortical sites responding to stimulation with an MEP. The cortical sites eliciting MEPs in a single muscle (either an oro-facial or a hand-forearm muscle) are denominated Single Positive Sites (SPs); the cortical sites eliciting responses in multiple muscles are defined as Multiple Positive Sites (MPs). Stimulation of MPs resulted in a simple muscle combination response (MPs–SMc) when activating several muscles within the same effector (oro-facial or hand-forearm) and in a complex muscle combination (MPs–CMc) when activating several muscles involving both the effectors (oro-hand responses).

the effectors simultaneously ("oro-hand responses"). We analyzed responses evoked by the minimum combination of stimulation parameters (intensity × number of pulses, cMT, see Fig. 2).

## Map of Positive Sites

For each patient, the reconstruction of the exact position of the Positive Sites over the cortex was computed. During intraoperative mapping, the entire exposed craniotomy was video recorded and the MRI coordinates of the Positive Sites were acquired by the neuronavigation system. To determine the exact position of the Positive Sites on the 3D MRI cortical surface of each patient, the following procedure was adopted. The postcontrast $T_1$-weighted sequence of each patient (the same loaded onto the neuronavigation system during surgery) was used to perform the cortical surface extraction and surface volume registration computed with the Brainsuite 15b dedicated software (Shattuck and Leahy 2002), and then the results were loaded into Brainstorm (MatLab Tool Box; Tadel et al. 2011), which is documented and freely available for download online under the GNU general public license (http://neuroimage.usc.edu/brainstorm).

With the aid of Brainstorm, the exact position of the Positive Site coordinates was marked on the patient's 3D MRI. Subsequently, the 3D MRI and the labeled Positive Sites were coregistered to the MNI space system (ICBM 152) with the aid of Brainstorm. The coordinates of each Positive Site were then entered into ICBM 152 to create a 3D reconstruction of the left (stimulated) hemisphere, and reported using a color code (Fig. 3A) based on the responsive muscle, to generate the somatotopic representation of effectors activated from both vlPM-BA6 and M1 (Fig. 3A). This analysis was performed in 19 out of 21 patients (total number of Positive Sites in M1 = 40 and in vlPM-BA6 = 46) where both the video and the navigation system recordings were available during cortical stimulation. A probabilistic map in the MNI coordinate system (Fig. 3B) was then obtained using MNI values of each Positive Site. Graphical reconstruction was performed with a dedicated script based on probability density function implemented in MatLab.

### *Analysis of MEPs*

During the procedure, MEPs elicited by DES were recorded with specific software (ISIS, INOMED, sampling rate 20 kHz, notch filter at 50 Hz). For each patient, the raw data, that is, all the MEPs recorded during the procedure, were extracted from the acquisition system and resampled at 4 kHz and analyzed offline by means of dedicated MatLab software. For each trial, a window of interest of 100 ms from the stimulus onset was defined. The average background EMG activity and its SD (±1 SD) were then calculated from the last 25 ms of the record (i.e., from 75 to 100 ms). An MEP was considered present if the response exceeded the average background ±1 SD, and its onset latency, duration, and amplitude were determined. Once extracted, MEPs were stored based on muscle and area (M1 vs. vlPM-BA6). Up to 24 muscles were recorded simultaneously. Following a careful analysis of all recorded muscles, we focused on responses in oro-facial muscles OO and MYLO and forearm-hand muscles EDC, FDI, APB, and ADM as defined above. No lower limb muscles were considered in the analysis, since no motor responses were ever elicited in the lower limb muscles by vlPM-BA6 stimulation (see also Cerri et al. 2015). Only MEPs obtained when the patients were fully awake were analyzed. We asked patients to lie still with all body parts at rest. The offline analysis was performed with great care to identify MEPs possibly contaminated/facilitated by voluntary movements.

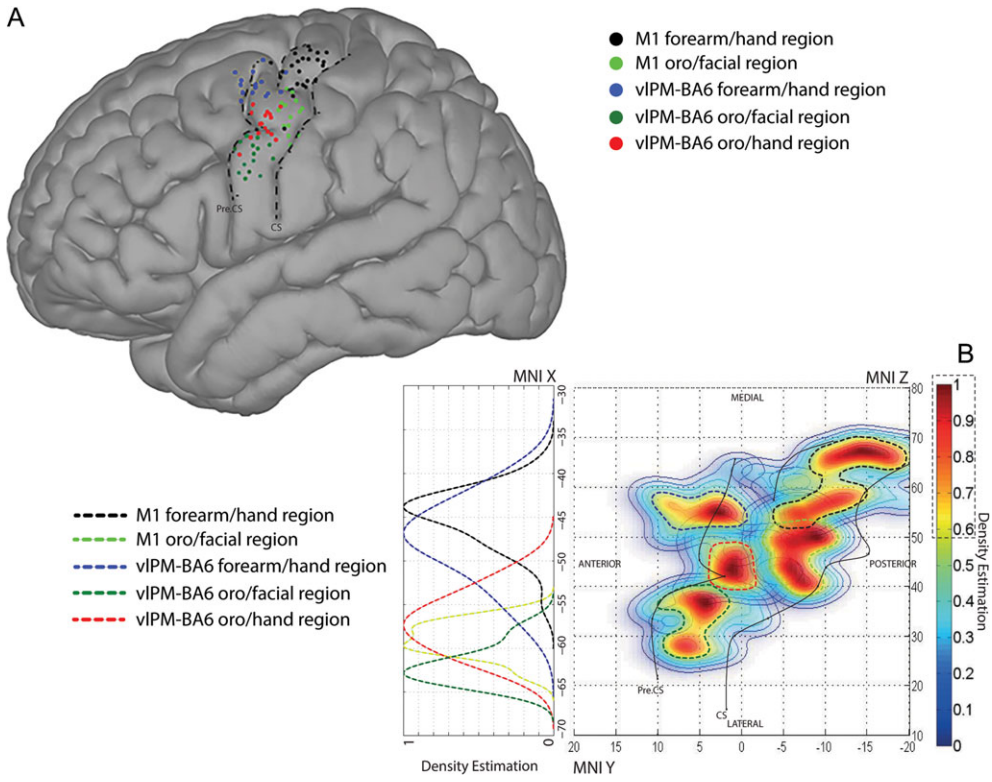


**Figure 3.** (*A*) MNI template (nonlinear ICBM 152); each dot represents a Positive Site and the color represents its somatotopic group. (*B*) Two-dimensional probabilistic map, based on the MNI coordinates (*X* and *Z*) for each site present in the MNI template and on the left hemisphere, showing the distribution for each somatotopic group of the *X* values in the site with the higher probability density value. Color bar represents the density estimation value. Colored dashed lines correspond to a specific somatotopic muscle group. In both (*A*) and (*B*), the central sulcus (CS) and precentral sulcus (PreCS) are indicated.

Visual inspection of any raw EMG activity allowed us to exclude all "preactivated" MEPs from the analysis.

The main parameters considered for the comparison between M1 and vlPM-BA6 were (A) "latency of MEPs" and (B) "cortical excitability" measured by the analysis of combination of the stimulation parameters (intensity and number of pulses) needed to elicit a motor response from each area.

*(A) Analysis of response latency: M1 versus vlPM-BA6.* For each MEP in each analyzed muscle, the "Absolute latency", that is, the delay between the "effective pulse" and the MEP onset was calculated. The intraoperative stimulation protocol included single pulse and/or trains of pulses (1–5 pulses with an ISI of 3–4 ms), depending on the clinical need, conditions, and purpose. In each subject, when an MEP was elicited with a single stimulus, which usually occurred for M1, and in almost 50% of trials for vlPM stimulation, the delay was easily computed between the stimulus artifact and the onset of the response (see above). When a train of pulses was applied, the "effective pulse," that is, the pulse within the train that actually induced motoneuron discharge and, in turn, the MEP, was calculated, as explained below, in 2 different situations, depending on the clinical constraints and needs. 1) During the mapping procedure, the surgeon started with one pulse and then increased the number of pulses until he reached the number of pulses capable of evoking an MEP. In this case, the last stimulus in the train eliciting an MEP was considered to be effective one. 2) During mapping, the surgeon used a train of 5 shocks without progressively increasing or reducing the number of pulses. In this case, it was possible to calculate the effective stimulus only by means of a probabilistic estimation applied at single trial level, using as a reference the latency of MEPs elicited with a single pulse to M1. The main assumption in this estimation was that, within a train of shocks delivered in vlPM, the MEP latency measured from the stimulus which was considered to be the effective one (e.g., the third in a train of 5 shocks), should be "equal" to, or "longer" than, but never "shorter" (in each case ± 1 SD) than the latency of the MEP in the same muscle evoked by a single pulse delivered to M1 in the same patient. Responses elicited from M1 were expected to be the fastest, due to its direct connections with motoneurons (Cerri et al. 2003; Shimazu et al. 2004) and its population of corticospinal neurons with the fastest conduction velocity (Firmin et al. 2014). Given these premises, patients without MEPs to single pulse from M1 were not included in this study.

According to this assumption, when MEPs were elicited with a train of pulses, the effective stimulus within each train was identified, selected and, accordingly, the latency of the evoked response estimated. The same analysis was applied for each muscle with responses from M1 and from vlPM-BA6 separately. In each subject, the analysis was performed for each stimulus trial.

*(B) Analysis of the cortical excitability: M1 versus vlPM-BA6.* This analysis was performed in order to reveal whether the 2 cortical areas showed different levels of excitability, defined as the combination of the minimum intensity and number of pulses necessary to evoke a response (cMT). Due to clinical constraints, it was not possible to assess, at each stimulated site, the minimum intensity and number of pulses necessary to

evoke an MEP. Two sets of data were available for analysis. In the "first analysis" (A), cortical excitability could be assessed from MEPs that were elicited from both areas by just a single pulse. This allowed for direct comparison between the 2 areas. This analysis was run separately for 9/12 patients with oro-facial responses and 8/12 with forearm-hand responses. In order to compare the excitability of the "pure" oro-facial and forearm-hand groups of the 2 areas, complex oro-hand responses were excluded.

In the "second analysis" (B), we examined MEPs that were evoked from both areas with trains of pulses. Given that it was not possible to assess, at each stimulated site, the minimum intensity and number of pulses necessary to evoke a threshold motor response, the excitability of the 2 areas was compared by assessing the combination of the intensity and the number of pulses needed to evoke MEPs of comparable amplitude from the 2 cortical areas. This procedure was applied for both groups of muscles. To this aim, a Z-score standardization of the raw amplitude within same muscle, independent of by area, was performed. Only trials with an amplitude Z-score included in a restricted range (–0.5/0.5) were selected for the analysis. Again, complex responses were excluded.

*Analysis of the cortical excitability within vlPM-BA6*. Thirty-five percent of responses obtained by stimulating vlPM-BA6 proved to be oro-hand responses, that is, complex responses involving muscles from 2 different effectors. These responses were rare when stimulating M1 (see above), where responses to one site of stimulation were recorded in one or more muscles belonging either to the forearm-hand "or" to the oro-facial group. Therefore, within vlPM-BA6 3 different groups of responses were identified: those with oro-hand responses, those with pure forearm-hand, and those with pure oro-facial responses. In order to compare the excitability within the vlPM-BA6 groups, the combination of the intensity and the number of pulses needed to evoke MEPs of comparable amplitude in the 3 groups was compared.

## Statistical Analysis

Statistical analysis was run to compare latency and excitability of MEPs evoked from vIPM-BA6 stimulation in oro-facial (MYLO and OO) and forearm-hand muscles (EDC, APB, FDI, and ADM).

### *Analysis of Response Latency: M1 Versus vlPM-BA6*

At the single subject level, a Student's *t*-test and Mann–Whitney *U*-test were used to assess statistical differences for different samples of muscles (oro-facial subsample, OO and MYLO; forearm-hand subsample, EDC, ADM, APB, and FDI). Separate analyses were carried out for responses obtained with a single pulse from those obtained with multiple pulses. We included only muscles for which data were available from at least 5 trials in both areas and in patients tested with the same condition (single and multiple pulses) for both areas. In order to compare homogeneous subsamples for both M1 and vlPM/BA6, we did not include responses from a muscle obtained from only 1 of the 2 areas.

At the population level, a Kolmogorov–Smirnov test showed that, within each group of muscles (oro-facial and forearm-hand), the latencies were normally distributed. Two different analyses were performed. In the "nonstandardized" analysis, the comparison of MEPs evoked from the 2 areas was performed using absolute latency, in ms. A Student's *t*-test was used when comparing paired sets of data, and the ANOVA test for analysis of data with >2 categories. For multivariate analysis of latency, a generalized linear model (GLM) analysis of variance was used to test the factor brain area (vlPM-BA6 and M1), muscle (oro-facial subsample and forearm-hand subsample), and patient variability. We included in the model interaction terms between independent variables. We performed post hoc tests using the Bonferroni correction. In the "standardized" analysis, we applied the same statistical procedure performed above on the latencies after conversion from ms to Z-score within each patient for each muscle independently by area, in order to minimize the possible discrepancies due to variation in length of conduction path due to different body size. Parallel to the single subject analysis, a Student's *t*-test was used to assess statistical differences for oro-facial subsample and forearm-hand subsample on the basis of number of the pulses applied (single pulse and multiple pulse).

### *Analysis of Cortical Excitability: M1 Versus vlPM-BA6*

Two types of analysis were undertaken. In Analysis A, we compared intensity differences for responses evoked from the 2 areas in the 2 groups of muscles with single-pulse stimulation. Univariate analysis was performed separately for oro-facial and forearm-hand muscle groups: a *t*-test was used when comparing paired sets of data and an ANOVA test for analysis of data with >2 categories. A multivariate analysis, GLM analysis of variance was performed independently by somatotopic cortical area, testing the correlation between brain area (vlPM-BA6 or M1), muscle and subject variability on the stimulus intensity used. Interaction terms between independent variables were included in the model. Post hoc tests were performed using the Bonferroni correction.

In Analysis B, we compared the intensity and the number of pulses needed to evoke MEPs of comparable amplitude from the 2 areas (vlPM-BA6 vs. M1) and within the different muscle groups. An initial analysis showed that there was no significant difference in the amplitude of the evoked responses from the 2 areas (M1 and vlPM-BA6), which were in a common range of amplitudes. A multivariate GLM analysis of variance was computed to test the correlation between brain area (vlPM-BA6 and M1), muscle group and patient variability on MEP amplitude in the oro-facial and forearm-hand group separately. A univariate analysis and a GLM analysis of variance were performed independently by muscle group, testing the impact of brain area (vlPM-BA6 or M1), muscle and subject variability on cortical excitability, defined as the intensity and number of pulses needed to elicit a response.

### *Analysis of Cortical Excitability Within vlPM-BA6*

Following the assessment of the inclusion criteria (see above Analysis B), a statistical analysis was performed to compare the intensity and the number of pulses needed to evoke MEPs of comparable amplitude in each group of muscles for vlPM-BA6 (pure forearm-hand, pure oro-facial, and oro-hand responses). A one-way ANOVA was used to compare quantitative data across 3 categories (forearm-hand, oro-facial, and oro-hand responses).

SPSS statistical software (IBM) version 20 was used for statistical analyses.

# Results

## Cortical Distribution and Features of Positive Sites in 21 Patients

MEPs from 49 sites in M1 and 48 in vlPM-BA6 (total 97 sites) were collected.

In M1: 26/49 Single Positive sites were identified that gave responses in a single muscle, 21/49 Multiple Positive sites, that is,

eliciting simple muscle combination responses within the same effector and 2/49 Multiple Positive sites, that is, eliciting "complex muscle combination responses" activating muscles belonging to different effector groups, so-called oro-hand responses (Fig. 2).

In vlPM-BA6: 18/48 Single Positive sites were identified, 13/48 Multiple Positive sites eliciting simple muscle combination responses, and 17/48 Multiple Positive sites eliciting complex muscle combination responses (Fig. 2).

By comparing the relative percentage of the 3 different response categories (single muscle responses, simple combinations, and complex combinations of muscle responses) evoked from the 2 regions, it appears that responses from M1 showed a clear prevalence of single muscle responses and simple combination muscle responses (53% and 43%, respectively), while responses from vlPM-BA6 showed all categories of response in equal proportions (38%, 27%, and 35%, respectively). It was rare to find complex muscle combinations evoked from M1 (4%).

A 3D reconstruction of the left hemisphere based on the final MNI template (ICBM 152) was computed to show the position of the Positive Sites in M1 and vlPM-BA6 and the somatotopic organization of the sites in the 2 areas (Fig. 3A). In M1, 2 distinct groups were identified: one, more medial, with a forearm-hand representation (black dots) and one, more lateral, with an oro-facial representation (light green dots). In vlPM-BA6, 3 different somatotopic representations were identified. The most ventral sector was almost exclusively an oro-facial group (dark green dots), while dorsally up to the inferior frontal gyrus pure forearm-hand responses (blue dots) were more prevalent. Located between these 2 groups a "transition zone" emerged, characterized by the presence of Multiple Positive sites eliciting complex muscle combinations, the 'oro-hand' responses. Stimulation of these cortical sites elicited motor responses with similar amplitude in several muscles of the forearm-hand and oro-facial groups simultaneously. As explained above, this category was almost absent in M1 and, in the few sites giving rise to such responses, there was a clear difference in amplitude, with forearm-hand motor responses always being larger than oro-facial. This result suggests that these sites are actually located in the M1 hand area right at the border with the M1 oro-facial area. When these cortical sites were stimulated, the pulse elicited clear hand responses and, probably, due to the spread of current to the neighboring oro-facial groups, evoked small oro-facial responses. These results in general clearly argue against an overlapping co-representation of both effectors in M1. Figure 3B shows the somatotopic probabilistic map (lateral view of the left stimulated hemisphere) obtained by means of MNI coordinates of each Positive Site. The density estimation for each site is reported with a color code indicating the probability level of site density obtained by interpolating MNI Y and Z values. Due to the tumor location and cortical surface made available by the flap during cortical mapping, we could not systematically investigate all regions in all patients. The actual localization of the sites in M1 and in vlPM-BA6 was confirmed by the analysis of the latency of the responses (see MEP Latency), which was critical in assigning the response as originating from M1 rather than from vlPM-BA6.

## MEP Latency

A total of 3595 MEPs were recorded, including 1931 trials from M1 stimulation and 1664 from vlPM-BA6. These MEPs were recorded in 6 muscles (300 ± 135.7 (SD) trials per muscle) in 21 subjects (33.7 ± 17.9 trials for each subject). In the forearm-hand group, 2452 trials were recorded, 1635 from M1, and 817 from vlPM-BA6.

Analysis at the single subject level was performed for 2 conditions: the single-pulse condition (10 patients) and the multiple-pulse condition (15 patients). We compared the latencies of MEPs from M1 and vlPM across muscles and conditions (single vs. multiple pulse). In both conditions, Student's *t*-test and *U*-test showed similar levels of significance ($P < 0.05$). In the single-pulse analysis, all but 2 patients in the oro-facial subsample, and 2 in forearm-hand subsample showed a statistical difference ($P > 0.05$) between the latencies of MEPs evoked from the 2 areas (see Fig. 4A). In the multiple-pulse analysis, all but one patient in the oro-facial subsample and one in the forearm-hand subsample showed statistical differences ($P < 0.05$).

At the population level, the nonstandardized univariate and multivariate analysis demonstrated that MEP latency in forearm-hand muscles from M1 was significantly shorter than in vlPM-BA6 (M1 = 22.4 ± 3.3 ms vs. vlPM-BA6 = 23.5 ± 3.0 ms; $P < 0.001$, see Supplementary Table 2) and the same result was confirmed within each subject ($P < 0.001$). The same analysis confirmed this result for the oro-facial subsample (M1 = 10.7 (±1.7 ms) versus vlPM-BA6 = 12.9 (±1.9 ms); $P < 0.0001$, see Supplementary Table 2).

Analyses using latencies standardized by Z-score were performed in order to remove intersubject variability in latency due to differences in body size and conduction distance (Livingston et al. 2010). Again, univariate and multivariate analysis showed that M1 had significantly shorter latencies than vlPM-BA6 for both forearm-hand muscles ($P < 0.001$, Supplementary Table 2) and oro-facial group ($P < 0.001$, Supplementary Table 2) (Fig. 5A). Univariate analysis performed for each muscle separately between areas again confirmed a significant shorter latency in M1 respect to vlPM ($P < 0.001$) (see Fig. 5B).

In the applied models, we included the latencies of MEPs obtained with a single pulse and those obtained with trains of stimulation. Given that it is not possible to exclude that the neural elements recruited with a single pulse could be different from those recruited with a train of pulses, we performed the same statistical analysis aimed at evaluating the latency shift (Z-scores) between M1 and vlPM-BA6 based on the stimulation paradigm, that is, separating data obtained with a single pulse and those obtained with a train of pulses. This analysis confirmed, for both single and multiple pulses, a statistical difference between M1 and vlPM-BA6 in both muscle groups ($P < 0.001$) (see Fig. 5C).

For single pulses, the latency difference for M1 versus vlPM evoked MEPs in oro-facial muscles ranged from 0.3 to 4.59 ms and in forearm-hand muscles from 0.8 to 5.22 ms. For a train of pulses, the latency differences were 0.47–2.44 ms for oro-facial and 0.19–7.38 ms for forearm-hand muscles (Fig. 4B).

From this analysis, it clearly emerges that vlPM-BA6 in the human brain has a motor output characterized by responses with a longer latency with respect to those originating from M1.

## Cortical Excitability Results

First, Analysis A was performed on data obtained with single pulses (10 out of 21 patients), with a total number of 1162 trials (354 in vlPM-BA6 and 808 in M1) grouping together OO and MYLO responses in the oro-facial (330 trials) group, and EDC, APB, FDI, and ADM in the forearm-hand (832 trials) group (average for each subject: 96.8 ± 118.3 trials). For this analysis, only MEPs evoked with a single stimulus at minimum current intensity were considered (see Materials and Methods): stimulus intensity was the only dependent variable and the 2 areas were compared with respect to this parameter.

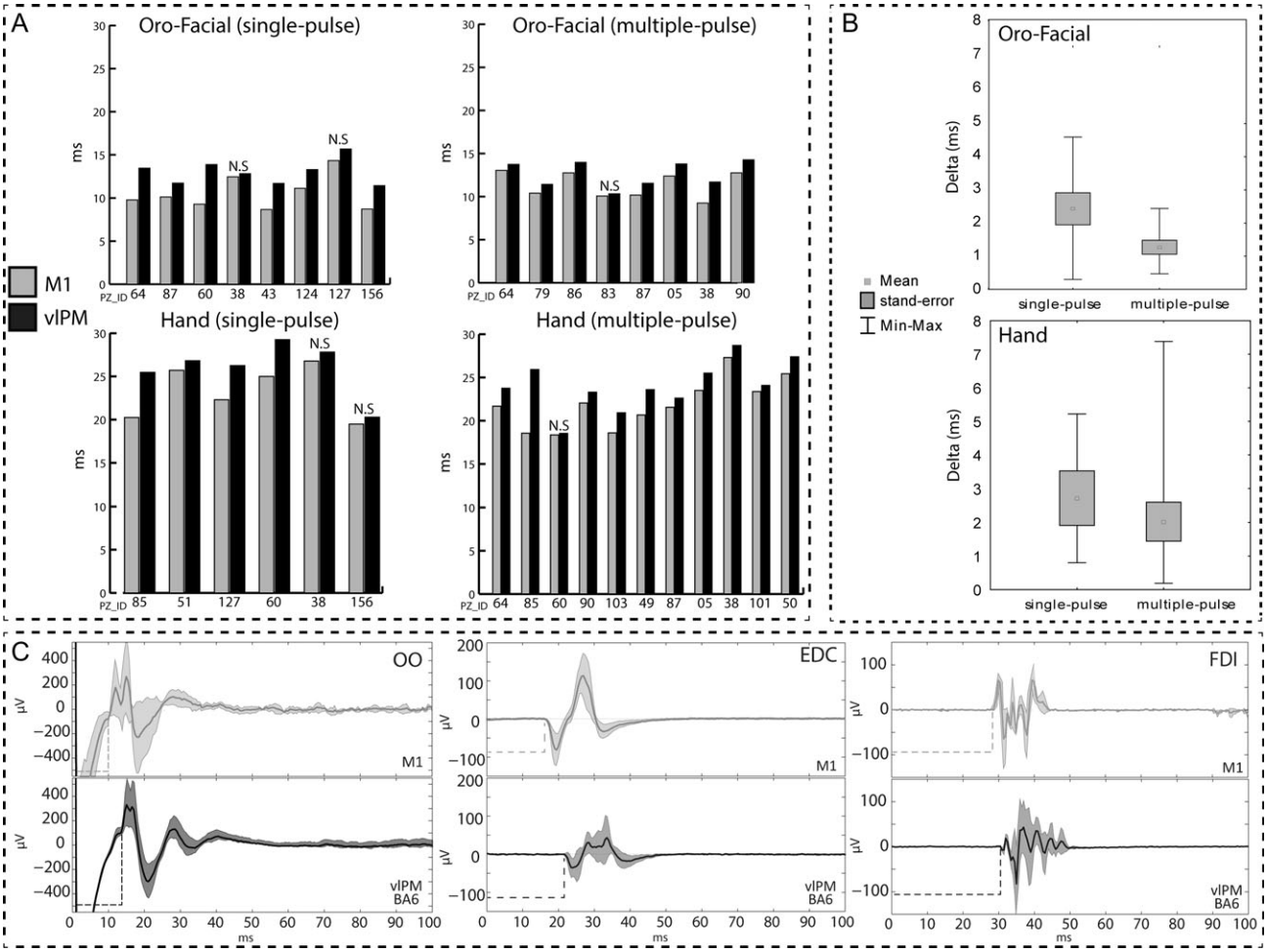


**Figure 4.** (A) Latency analysis of MEPs obtained with single and multiple pulses in oro-facial and forearm-hand muscles at the single subject level. NS indicates that the difference between the latency of responses to M1 and vlPM stimulation was not significant. (B) Mean latency differences ("Delta ms") of MEPs evoked from vlPM and M1 with single and multiple pulses calculated for each patient and for each group of muscles. Average value, standard error, and min/max of Delta (in ms) are shown. (C) Examples of averaged MEPs with SDs (10 trials, single pulse) from 3 muscles evoked by stimulation of vlPM-BA6 and of M1 in patient 51 (EDC and FDI) and in patient 64 (OO). Dashed lines indicate the latency between the stimulus and the rising phase of the MEP.

Univariate analysis revealed that the stimulus intensity needed to obtain a significant MEP (see Materials and Methods) from the forearm-hand group was significantly higher for vlPM-BA6 (15.98 mA) compared with M1 (10.33 mA) ($P < 0.001$, see Supplementary Table 2), but it was not significantly different for the oro-facial group (23.94 mA in vlPM-BA6 vs. 22.72 mA in M1; $P = 0.311$, Supplementary Table 2) (Fig. 6A).

Second, Analysis B estimated the combination of stimulus intensity and number of pulses needed to evoke MEP responses of comparable amplitude from vlPM-BA6 and M1. Inclusion criteria were satisfied in 15 patients out of 21, for a total of 503 trials in vlPM-BA6 and 455 in M1 (293 in the oro-facial group and 665 in the forearm-hand group, mean trials for each subject = 59). The overall amplitude of MEPs in forearm-hand and in oro-facial groups was comparable for responses evoked from M1 and vlPM-BA6 (respectively $P = 0.47$ and $P = 0.75$, Supplementary Table 2) and the same was true at the individual patient level for both oro-facial and forearm-hand groups (respectively $P = 0.29$ and $P = 0.95$). Based on this assumption, the combination of intensity and number of pulses needed to elicit motor responses of comparable amplitude between both regions was analyzed.

Univariate analysis of stimulus intensity confirmed that the intensity needed to evoke an MEP was significantly higher in vlPM-BA6 than M1 for the forearm-hand group ($P < 0.001$, Supplementary Table 2), but not for the oro-facial group ($P = 0.28$, Supplementary Table 2).

Univariate analysis of the number of pulses showed that the number needed to evoke an MEP was significantly higher for vlPM than M1 for the oro-facial group ($P < 0.001$, Supplementary Table 2), but not for the forearm-hand group ($P = 0.12$, Supplementary Table 2).

In the multivariate models, we found that brain area was a significant predictor of the model for the intensity ($P < 0.001$), but not for number of pulses ($P = 0.64$).

The results of the 2 different analyses (Analyses A and B) globally showed that MEPs from vlPM-BA6 required a higher intensity of stimulation with respect to M1, in the forearm-hand group, but not in the oro-facial group. The number of pulses seems to be less relevant in distinguishing the excitability of the 2 areas (Fig. 6B).

A dedicated analysis of excitability was performed within vlPM-BA6 in order to compare the excitability of the 3 different somatotopic regions (forearm-hand, oro-hand, and oro-facial)

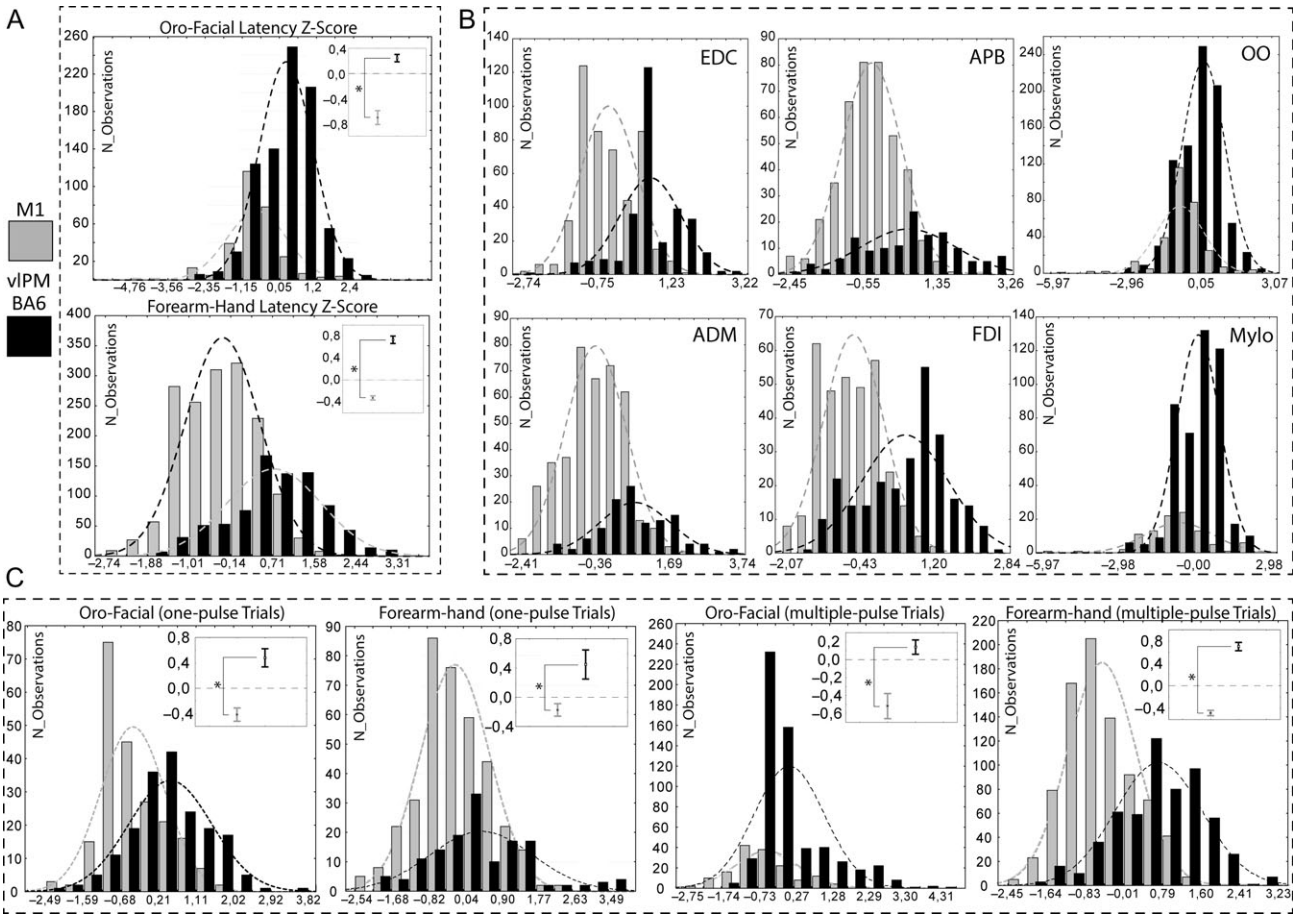


**Figure 5.** (*A*) Distribution of latencies of MEPs evoked from the 2 cortical areas in oro-facial and forearm-hand muscle groups. In order to show the distribution at population level, the latencies in ms were standardized as *Z*-scores within each patient and for each muscle by area stimulated. This minimized possible discrepancies in absolute latencies due to variation in conduction distance with overall different body size. The dashed line represents the normal distribution of the MEP latencies expressed as a *Z*-score. In each figure, the right-upper panel shows box plots with mean value and standard error for MEP latencies evoked from each area. (*B*) Distribution of the *Z*-scored latencies of MEPs evoked from the 2 areas in each muscle. (*C*) Distribution of the *Z*-scored latencies of MEPs evoked from the 2 areas with single-pulse stimulation and multiple-pulse stimulation in oro-facial and forearm-hand muscles.

represented in this area. For this analysis, responses of comparable amplitude obtained by stimulating the 3 vlPM-BA6 regions were selected and the same criteria as for Analysis B were adopted. In all, 21 patients were included: 194 oro-facial trials (15 patients), 361 oro-hand trials (9 patients), and 310 forearm-hand trials (9 patients) with and average number of trials for each subject of about 41.

Multivariate analysis showed that the amplitude of the responses was not different in the different somatotopic groups, whether oro-facial, oro-hand, and forearm-hand ($P = 0.6$, Supplementary Table 2), thus confirming the inclusion criteria. Results showed that both intensity ($P < 0.001$) and number of pulses ($P < 0.001$, Supplementary Table 2) needed to elicit comparable responses in the 3 groups were found to be significantly different, suggesting a nonhomogeneous distribution of the excitability within vlPM-BA6.

Univariate analysis was then performed among the groups. The main results revealed that the oro-hand and the forearm-hand groups showed a difference in excitability, reflected not by number of pulses ($P > 0.05$), but by the intensity of current ($P < 0.05$) needed to evoke a response (Fig. 6C). It is difficult to interpret the excitability of the oro-facial group, since both number of pulses and intensity show significant differences respect to the other muscle groups, but in the opposite direction.

## Discussion

In this study, the somatotopic organization of motor output from left ventrolateral (vlPM-BA6) human premotor cortex was investigated during intraoperative mapping, which allows a unique stimulation approach of the exposed cortex during surgery for brain tumor removal. Stimulation with short trains of HF pulses was applied over the left vlPM-BA6, and MEPs evoked in forearm-hand and oro-facial muscles were recorded and compared with those obtained by stimulating M1. By means of this analysis, the somatotopic organization and the distinguishing features of the motor output from these 2 cortical areas were revealed.

### Somatotopic Organization of the Motor Output in the Human Left vlPM-BA6

In nonhuman primates the somatotopic organization of M1, and that of the dorsal and the ventral premotor cortex (dPM and vPM) has been revealed by anatomical and electrophysiological investigations (Dum and Strick 2005; Boudrias et al. 2010a, 2010b).

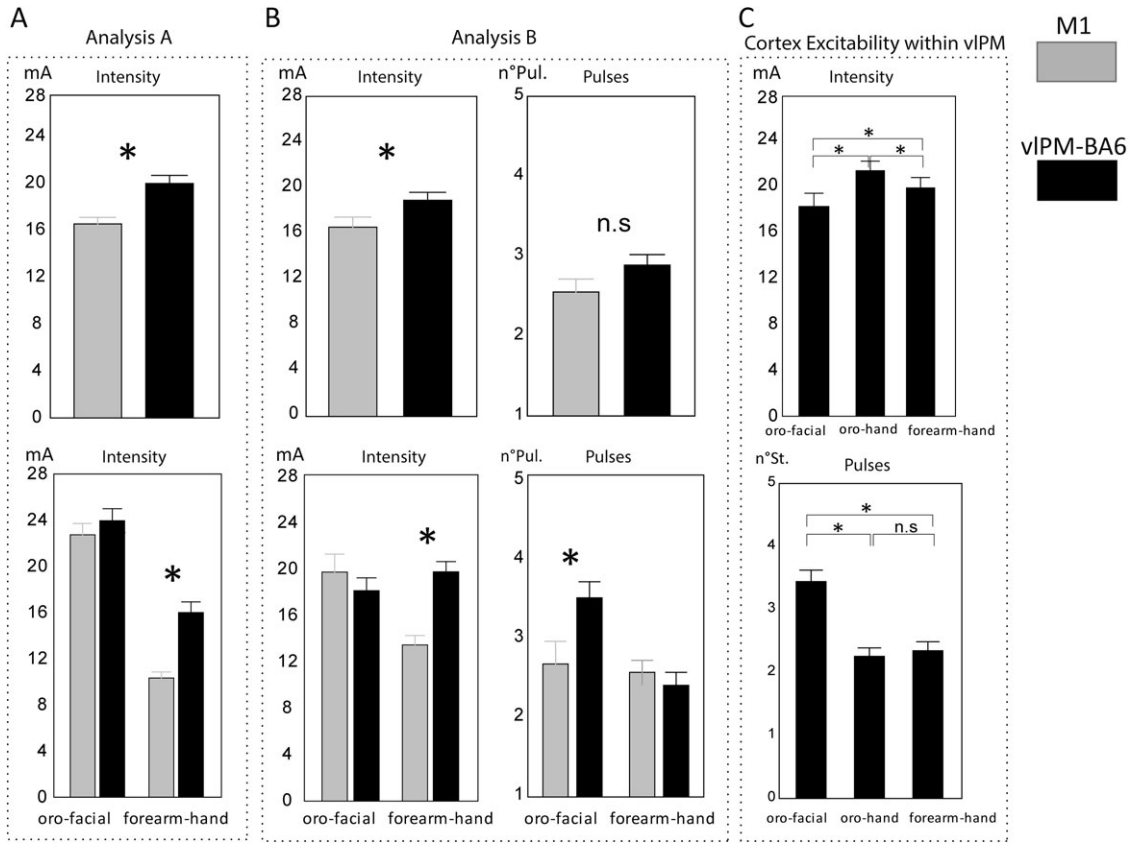


**Figure 6.** (A) Comparison of cortical excitability (Analysis A). Upper panel: the bar graph with standard errors represents results obtained by multivariate analysis of differences in intensity (in mA) between vlPM-BA6 and M1. Lower panel: results of the univariate analysis of differences in intensity (in mA) between vlPM-BA6 and M1 for each muscle group. (B) Comparison of cortical excitability (Analysis B). Upper panel: the bar graph with standard error represents results obtained from the multivariate model concerning differences in intensity (in mA) and number of pulses (n°Pul) between vlPM-BA6 and M1. Lower panel: results of the univariate analysis of differences in intensity (in mA) and number of pulses (n°Pul) between vlPM-BA6 and M1 for each muscle group. (C) Excitability of different subdivisions of vlPM-BA6. Above, bar graph showing differences in intensity (in mA) and below, number of pulses (n°Pul) for the 3 types of responses evoked from different somatopic regions of vlPM-BA6 (oro-facial, oro-hand, and forearm-hand). In all bar graphs, asterisks indicate significant differences, $P < 0.05$.

Although these studies provide a fundamental reference for investigation of vPM in humans, where a clear-cut description of the anatomo-functional subdivision of the premotor cortex is lacking, it is likely that the human premotor cortex shows some differences due to the increased complexity of the human sensorimotor system. ICMS, retrograde labeling, and single unit recording from macaque brain have shown that outputs to a single muscle are represented multiple times over a wide region of the motor cortex in a complex, mosaic fashion (Andersen et al. 1975; Porter and Lemon, 1993; Rathelot and Strick 2006, 2009; Boudrias et al. 2010a, 2010b). Human fMRI studies have confirmed this multiple, overlapping structure of motor outputs (Sanes et al. 1995; Schieber 2001). Based on this organization, it has been suggested that when a complex movement is to be performed, the horizontal connections within the motor cortex link ensembles of neurons that coordinate the ultimate pattern of discharge of the spinal motoneurons driving the different muscles needed to perform the planned movement (Lemon 1988; Porter and Lemon 1993; Barinaga 1995; Schieber 2001).

Our study used intraoperative stimulation during tumor removal to investigate the motor output of vlPM and M1. To this aim, the motor responses elicited in the same sample of muscles recorded simultaneously when mapping the 2 cortical areas under the same conditions were compared. The results show that Single Positive sites—cortical sites that, when stimulated, activated a single muscle among those recorded—are more common in M1 than in vlPM (Fig. 2; 53% vs. 38%). The more focused muscle representation in M1 is consistent with the idea of a surround inhibition in the fields around the stimulated spot, mediated through GABAergic transmission, potentially important for selective execution of desired movements (Mink 1996; Ziemann et al. 1996; Sohn and Hallett 2004). However, voluntary execution of movements, even those involving a single digit, are rarely isolated contractions of one muscle, but require simultaneous control of many different hand and forearm muscles acting on different fingers and joints (Schieber 1991). Pyramidal neurons in the motor cortex exert excitatory influences on their postsynaptic targets via their intracortical axon collaterals synapsing on other pyramidal neurons, as well as on cortical inhibitory interneurons (Hendry and Jones 1981; Markram et al. 1998; Silberberg and Markram 2007). The connections between pyramidal neurons provide feedforward excitatory interactions between groups of cells related to the same movement, whereas the connections with inhibitory interneurons may form a basis for surround inhibition between cortical zones related to the activation of different muscles (Keller and Asanuma 1993). When comparing the 2 areas, it may be that in M1 the distribution of excitability (due to the peculiar architecture of surrounding inhibition), is

such that the stimulation of a complex and overlapping muscle representation, can still emerge as a single muscle response, reflecting the net strength of outputs to that particular muscle when compared with those of other neighboring muscles (some of which were not monitored in our study). The excitability in vlPM-BA6 may be distributed in a different fashion, allowing the emergence of similarly weighted outputs to multiple muscles.

In M1 the number of Single Positive sites was higher in the forearm-hand group than in the oro-facial group (70% forearm-hand vs. 30% oro-facial), while in vlPM-BA6 an equal percentage of such sites was found in both forearm-hand and oro-facial groups. The different proportion of single upper limb versus cranial muscle response found in M1 could reflect a particular role of the human M1 in controlling hand movement. However, since M1 is mainly located within the bank of the central sulcus, particularly the more caudal 'new' M1 (Geyer et al. 1996; Rathelot and Strick 2009) our result could reflect the particular difficulty of activating the oro-facial region of M1 with a stimulating probe on the cortical surface. It may also be that oro-facial and forearm-hand neurons are differentially sensitive to DES of the cortical surface. In contrast, in vlPM-BA6 both the oro-facial and the forearm-hand representations are located on the convexity of the precentral gyrus, and therefore both are more accessible to DES.

When considering the forearm-hand group in vlPM-BA6, the sampled muscles most often yielding MEPs were EDC and APB, followed by FDI, consistent with the role in grasp of the ventral premotor area (F5) in monkeys (Raos et al. 2006; Umiltà et al. 2007). During hand grasp, the EDC and the APB muscles are responsible for preshaping and opening of the hand, while the FDI muscle is fundamental in characterizing the type of grip, in particular the precision grip (Brochier et al. 2004). Accordingly, the reversible inactivation of the monkey F5 area impairs hand shaping preceding the actual grasp and the hand-posture relative to object size and shape (Fogassi et al. 2001). In humans, neuroimaging data show a significant engagement of motor areas, and in particular, the ventral sector of the premotor cortex, in highly skilled movement such as precision grip and haptic manipulation (Binkofski et al. 1999; Ehrsson et al. 2001). This feature could be reflected in the dominant representation in vlPM-BA6 of neurons controlling coordination of muscles such as EDC, APB, and FDI for precision grasp.

In contrast, a less dexterous grasp, such as a whole hand grasp or power grip that involves all hand muscles used in a less fractionated pattern, is known to be a less effective in fMRI-based activation of the human vPM (Ehrsson et al. 2000; Begliomini et al. 2007). Interestingly, one of the muscles contributing to this grasp, the ADM, was not found among vlPM-BA6 Single Positive sites. During intraoperative mapping, many Multiple Positive sites were disclosed, including also ADM. When stimulated, these sites elicited 2 types of responses: 1) simple muscle combination responses (MPs–SMc)—activating several muscles within same effector—and 2) complex muscle combination response (MPs–CMc)—activating several muscles from both, mouth and hand, effectors (oro-hand responses). Such multiple responses were more prevalent in the vlPM-BA6 than in M1 (62% vs. 47%), suggesting a more complex motor organization of this area with respect to M1. Multiple Positive sites found in M1 evoked co-contraction of multiple muscles within the same effector (OO and MYLO, EDC and ADM, FDI and ADM or all hand muscles), while the Multiple Positive sites in vlPM-BA6 elicit mostly oro-hand responses, that is, co-activation of 3 or all forearm-hand muscles and oro-facial muscles. These muscle combinations are almost exclusive features of the vlPM-BA6 (35% in vlPM-BA6 vs. 4% in M1), emerging as a distinctive group clearly segregated between a dorsal forearm-hand representation and a ventral oro-facial representation, as indicated by the 3D reconstruction (Fig. 3A, B).

One of the main hypotheses about vPM is its role in "goal-dependent control" of the hand, working as a fundamental "hub" encoding abstract components of the motor program, as opposed to the executive muscle patterns needed to achieve it (Bonini et al. 2011). The complex combination responses described here, never described previously from intraoperative investigations, highlight the complexity of organization within vlPM-BA6, which are consistent with these suggestions, but of course do not provide direct evidence of goal-oriented function.

## Connection to the Spinal Cord: Latency of Motor Responses

Anatomical studies in the nonhuman primate (Dum and Stick 1991, 2005) have shown that premotor areas, including vPM and dPM contribute to the corticospinal tract. However, these projections, in comparison with M1, show significant differences in terms of numbers, size, and spinal targets (Shimazu et al. 2004; Borra et al. 2010; Firmin et al. 2014), raising questions about their function in motor control. Functional imaging and DTI investigations in humans (Verstynen et al. 2011) have so far not resolved this issue. Electrical stimulation of M1 in the nonhuman primate evokes different descending volleys recordable in the pyramidal tract, an early D-wave, which reflects the direct electrical activation of corticospinal axons (Patton and Amassian 1954), and subsequent indirect waves, with an approximate interwave delay of 1.5 ms, considered to reflect trans-synaptic activation, via cortical interneurons, of corticospinal cells (Amassian et al. 1987). M1 stimulation elicits early motor responses consistent with D-waves leading to monosynaptic excitation of spinal motoneurons (Porter and Lemon, 1993; Maier et al. 2002; Shimazu et al. 2004). Conversely, there is no evidence that stimulating vPM gives rise to either a D-wave in the corticospinal tract or early motor responses (Shimazu et al. 2004; Maier et al. 2013), suggesting that the connections of this area with the spinal cord must be indirect and involve, for example, specific cortico-cortical connections with M1, which in turn sends numerous direct projections to spinal motoneurons of hand and forearm muscles (Morecraft et al. 2013). Alternatively, or in addition, corticospinal projections from vPM could recruit high-cervical propriospinal neurons (Borra et al. 2010). A powerful facilitation exerted by vPM on M1 motor output was clearly demonstrated in the macaque (Cerri et al. 2003; Shimazu et al. 2004), suggesting that the M1 hand area may be a critical hub in mediating vPM motor-related activation of spinal motoneurons (Schmidlin et al. 2008). This relatively complex and indirect pathway may well explain the higher intensities needed to elicit a motor output from the vPM compared with M1 (Cerri et al. 2003). Higher intensities are also needed to evoke motor responses from dPM (Raos et al. 2004).

When comparing data recorded in nonhuman primates with the data presented here, the constraints of the human intraoperative method must be discussed. To begin with, DES was delivered to the cortical surface while in the monkey it is normally delivered intracortically. Moreover, while the clinical procedure allowed recording the EMG activity from several hand and oro-facial muscles (both ipsi- and contralateral), it was not possible to monitor descending spinal volleys or directly investigate motoneuronal responses.

We compared the latency of MEPs elicited by DES of the 2 cortical areas in the same set of muscles, both at single subject and at population levels. The main result, in the great majority of patients tested, was that MEPs elicited from vlPM-BA6 had significantly longer latencies than those from M1. This main result was found both for responses obtained with single shocks and with trains of shocks, suggesting that our method of inferring the effective pulse within a train of 2 to 5 pulses was reliable (Materials and Methods; see Fig. 5). This significant difference in the latency of vlPM-BA6 versus M1 MEPs argues against the responses evoked from vlPM-BA6 being due to current spread from M1, but rather suggests that these MEPs originated from vlPM-BA6 itself. When observing the distribution of response latencies of MEPs evoked from vlPM-BA6 and M1, 2 different distributions emerged, although with a partial overlap (Fig. 5). Among the 2 areas, small differences in latency (<2 ms) as well as considerably larger differences (up to 5–7 ms) were observed, possibly underlying different pathways mediating responses evoked from the 2 areas. By considering only the average mean values, these nuances may be lost; in addition, the method used to estimate the effective pulse in a train may actually underestimate latency differences. The responses from vlPM-BA6 which had latencies only slightly shorter than those from M1 might be conducted by corticospinal fibers which are probably more slowly conducting than the fastest M1 fibers (Vigneswaran et al. 2011; Firmin et al. 2014), whereas those with greater latency differences (2.5–4.0 ms) might be mediated by a cortico-cortical interaction with M1, as in the macaque (Shimazu et al. 2004).

In any event, as in the macaque monkey, our results speak against a fast, direct excitation exerted by vlPM-BA6 on hand motoneurons comparable with the output from M1. Given the strong, bilateral and reciprocal connections between the premotor cortex and the primary motor cortex, it is essential to investigate the functional properties of the vlPM-BA6 regions that make cortico-cortical connections with M1 versus corticospinal projections to the cervical spinal cord, and their involvement in active motor control of the hand.

MEPs evoked in oro-facial muscles by vlPM-BA6 stimulation also showed a significantly longer latency than those elicited from M1 (Fig. 5). Despite the evidence, in macaques, for direct projections from vPM to the trigeminal and facial motor nuclei innervating the orbicularis oris and mylohyoid muscles (Simonyan and Jürgens 2003), the significantly longer latency observed for MEPs from vlPM versus M1 might suggests that, in humans, direct projections are unlikely to be engaged in the direct control of brainstem nuclei. For practical reasons, we could not record from laryngeal muscles, so cannot shed light on whether vlPM controls these muscles in humans.

Recently, DTI has been utilized to trace premotor descending fibers (Verstynen et al. 2011). Interestingly, the majority of descending fibers originating in the ventral sector of BA6 are shown to be located between BA44 and BA3 of S1, just above the lateral sulcus in a relatively concentrated area. Surprisingly, the cortical region reported by Verstynen et al. (2011) as the main premotor source of descending fibers did not coincide with our reconstruction maps plotting the premotor sites eliciting a clear motor output The discrepancy between our data and the neuroimaging data challenges the complete reliability of the DTI data and highlights the need to confirm the neuroimaging data with electrophysiological recording, in order to create a reliable human model. It should be pointed out that DTI shows the totality of the corticofugal fibers descending to the level of the cerebral peduncle, without identifying specifically corticobulbar or corticospinal fibers, which actually probably make up just a small percentage of the total corticofugal output (Tomasch 1969). The constraints of this technique do not yet allow the precise identification of how corticofugal components, originating from the different cortical areas, terminate at brainstem and spinal levels. In particular, the functional connectivity of the ventral premotor cortex with the spinal cord in humans remains obscure. However, anatomical studies suggest a clear role of this area in modulating the intrinsic spinal excitability and in recovery after lesion involving M1 (Schultz et al. 2012, 2014).

## Connection to the Spinal Cord: Cortical Excitability

DES over the cortical convexity allows a direct comparison of the excitability of vlPM with M1. Experimental studies have shown that the threshold current for activating cortical axons depends on both the axon size and the degree of myelination (Stoney et al. 1968). Increasing the intensity of the current leads to the activation of a greater number of axons within the stimulated region (spatial summation) and recruitment of an even greater population of neurons through functional synaptic connections made by these axons (Borchers et al. 2012; Maier et al. 2013). In addition to the intensity of the stimulation, the number of pulses applied also influences the neuronal excitability, by inducing temporal summation of the synaptic input to corticofugal cells. For this reason, it is unlikely that single pulse and trains of pulse act in the same way. We assessed the relative excitability of M1 with vlPM-BA6 by comparing the intensity of the DES current delivered, and the number of pulse required to evoke motor responses of similar amplitude.

The first analysis of stimulus intensity (Analysis A; see Materials and Methods) confirmed that vlPM-BA6 was less excitable than M1. The average intensity required to elicit responses to a single pulse in vlPM-BA6 was 20 mA and decreased when using trains of 2–5 pulses. The average intensity in M1 for both single and trains of pulses was comparably around 16 mA. The M1-vlPM difference was particularly marked for forearm-hand MEPs, but did not apply to oro-facial MEPs (Fig. 6).

In the second analysis (Analysis B), both the intensity and the number of pulse were considered. This analysis substantially confirmed the higher excitability of M1 with respect to the vlPM-BA6, but no significant differences in terms of stimulus number were found. The intensity emerges as the key factor determining cortex excitability. However, at subgroup level, the oro-facial and forearm-hand muscles showed differing results: the former showed similar intensities for both areas, but a difference in the number of pulse required, while the opposite was true for the forearm-hand subsample. In both, the statistical differences confirmed lower excitability of vlPM with respect to M1. The opposite trend could have been explained by a different strategy of stimulation applied during the surgery for the 2 subsamples of muscles, which is the reason why we analyzed them separately.

Our results resonate with those obtained with ICMS in non-human primate cortex, which have shown that motor outputs from dorsal and ventral premotor cortex are less excitable than from M1 (Cerri et al. 2003; Raos et al. 2003; Shimazu et al. 2004; Boudrias et al. 2010a, 2010b). However, ICMS threshold currents are typically in the order of 5–30 μA, much lower than those reported here with DES. The focused, intracortical location of the intracortical probe contrasts with intraoperative monopolar stimulation applied to the pial surface, with inevitable shunting of applied current over the wet cortex.

Interestingly, analysis of the excitability within the 3 somatotopic groups (pure forearm-hand, pure oro-facial, and oro-hand representation) in vlPM-BA6 revealed a sort of "excitability gradient." In particular, the oro-hand subsector showed a lower excitability with respect to the more dorsal forearm-hand subsector, consistent with data obtained in nonhuman primates reporting a relative inhomogeneity in the excitability within different subdivisions of vPM. In particular, sector F5c is reported to be less excitable with respect to the adjacent sector F5p, requiring higher current intensity to elicit movements (Maranesi et al. 2012). In the nonhuman primate, F5c neurons encode information mainly related to the observation of actions performed by others (Gallese et al. 1996). Recently, it has been reported that some of the corticospinal neurons in macaque vPM show mirror neuron features (Kraskov et al. 2014). Interestingly, many of them suppress their firing rate during action observation, although firing intensely during the monkey's own grasp, and it has been suggested that they constitute part of a cortical mechanism responsible for the inhibition of the self-movement during action observation (Kraskov et al. 2014).

## Conclusion

Thanks to the unique direct approach to the human brain allowed by the brain mapping technique during intraoperative investigation, this study demonstrates important differences in motor output between vlPM-BA6 and M1. Similarly to other nonhuman primates, human vlPM-BA6 is a less excitable area and motor responses evoked by electrical stimulation of this area have significantly longer latencies than those evoked from M1. This suggests that, as in the monkey model, vlPM acts via a slower and possibly more indirect route to the spinal cord. Whether these connections involve both cortico-cortical and corticospinal projections is still to be defined. Further investigations are necessary to confirm these findings for the right vlPM-BA6 in left- and right-handed patients, and to correlate the properties of the human vlPM-BA6 revealed by DES to natural, voluntary movements such as speech and the haptic manipulation of objects.

## Funding

Italian Ministry of Health, Ricerca Finalizzata (RF-2010-2309748 to L.B. and G.C.).

## Notes

The authors are deeply grateful to A. Castellano and V. Blasi for routine fMRI and DTI analysis. *Conflict of Interest*: None declared.

## References

Amassian VE, Stewart M, Quirk GJ, Rosenthal JL. 1987. Physiological basis of motor effects of a transient stimulus to cerebral cortex. Neurosurgery. 20:74–93.

Andersen P, Hagan PJ, Phillips CG, Powell TP. 1975. Mapping by microstimulation of overlapping projections from area 4 to motor units of the baboon's hand. Proc R Soc Lond B Biol Sci. 188:31–36.

Barinaga M. 1995. Remapping the motor cortex. Science. 268: 1696–1698.

Begliomini C, Wall MB, Smith AT, Castiello U. 2007. Differential cortical activity for precision and whole-hand visually guided grasping in humans. Eur J Neurosci. 25:1245–1252.

Bello L, Acerbi F, Giussani C, Baratta P, Taccone P, Songa V. 2006. Intraoperative language localization in multilingual patients with gliomas. Neurosurgery. 59:115–125.

Bello L, Riva M, Fava E, Ferpozzi V, Castellano A, Raneri F, Pessina F, Bizzi A, Falini A, Cerri G. 2014. Tailoring neurophysiological strategies with clinical context enhances resection and safety and expands indications in gliomas involving motor pathways. Neuro Oncol. 16:1110–1128.

Binkofski F, Buccino G, Posse S, Seitz RJ, Rizzolatti G, Freund H. 1999. A fronto-parietal circuit for object manipulation in man: evidence from an fMRI-study. Eur J Neurosci. 11:3276–3286.

Bonini L, Serventi FU, Simone L, Rozzi S, Ferrari PF, Fogassi L. 2011. Grasping neurons of monkey parietal and premotor cortices encode action goals at distinct levels of abstraction during complex action sequences. J Neurosci. 31:5876–5887.

Borchers S, Himmelbach M, Logothetis N, Karnath HO. 2012. Direct electrical stimulation of human cortex—the gold standard for mapping brain functions? Nat Rev Neurosci. 13: 63–70.

Borra E, Belmalih A, Gerbella M, Rozzi S, Luppino G. 2010. Projections of the hand field of the macaque ventral premotor area f5 to the brainstem and spinal cord. J Comp Neurol. 518:2570–2591.

Boudrias MH, Lee, Svojanovsky S, Cheney PD. 2010a. Forelimb muscle representations and output properties of motor areas in the mesial wall of rhesus macaques. Cereb Cortex. 20:704–719.

Boudrias MH, McPherson RL, Frost SB, Cheney PD. 2010b. Output properties and organization of the forelimb representation of motor areas on the lateral aspect of the hemisphere in rhesus macaques. Cereb Cortex. 20:169–186.

Breshears JD, Molinaro AM, Chang EF. 2015. A probabilistic map of the human ventral sensorimotor cortex using electrical stimulation. J Neurosurg. 123:340–349.

Brochier T, Spinks RL, Umilta MA, Lemon RN. 2004. Patterns of muscle activity underlying object-specific grasp by the macaque monkey. J Neurophysiol. 92:1770–1782.

Cerri G, Cabinio M, Blasi V, Borroni P, Iadanza A, Fava E, Fornia L, Ferpozzi V, Riva M, Casarotti A, et al. 2015. The Mirror Neuron System and The Strange Case of Broca's Area. Hum Brain Mapp. 36:1010–1027.

Cerri G, Shimazu H, Maier MA, Lemon RN. 2003. Facilitation from ventral premotor cortex of primary motor cortex outputs to macaque hand muscles. J Neurophysiol. 90:832–842.

Coudè G, Ferrari PF, Rodà F, Maranesi M, Borelli E, Veroni V, Monti F, Rozzi S, Fogassi L. 2011. Neurons controlling voluntary vocalization in the macaque ventral premotor cortex. PLoS One. 6 (11):e26822.

Dum RP, Strick PL. 1991. The origin of corticospinal projections from the premotor areas in the frontal lobe. J Neurosci. 11: 667–689.

Dum RP, Strick PL. 2002. Motor areas in the frontal lobe of the primate. Physiol Behav. 77:677–682.

Dum RP, Strick PL. 2005. Frontal lobe inputs to the digit representations of the motor areas on the lateral surface of the hemisphere. J Neurosci. 25:1375–1386.

Ehrsson HH, Fagergren A, Jonsson T, Westling GR, Johansson RS, Forssberg H. 2000. Cortical activity in precision- versus power-grip tasks: an fMRI study. J Neurophysiol. 83:528–536.

Ehrsson HH, Fagergren A, Forssberg H. 2001. Differential fronto-parietal activation depending on force used in a precision grip task: an fMRI study. J Neurophysiol. 85:2613–2623.

Ferrari PF, Gallese V, Rizzolatti G, Fogassi L. 2003. Mirror neurons responding to the observation of ingestive and

communicative mouth actions in the monkey ventral premotor cortex. Eur J Neurosci. 17:1703–1714.
Ferri S, Peeters R, Nelissen K, Vanduffel W, Rizzolatti G, Orban GA. 2015. A human homologue of monkey F5c. Neuroimage. 111:251–266.
Firmin L, Field P, Maier MA, Kraskov A, Kirkwood PA, Nakajima K, Lemon RN, Glickstein M. 2014. Axon diameters and conduction velocities in the macaque pyramidal tract. J Neurophysiol. 112:1229–1240.
Fogassi L, Gallese V, Buccino G, Craighero L, Fadiga L, Rizzolatti G. 2001. Cortical mechanism for the visual guidance of hand grasping movements in the monkey. A reversible inactivation study. Brain. 124:571–586.
Gallese V, Fadiga L, Fogassi L, Rizzolatti G. 1996. Action recognition in the premotor cortex. Brain. 119:593–609.
Geyer S, Ledberg A, Schleicher A, Kinomura S, Schormann T, Bürgel U, Klingberg T, Larsson J, Zilles K, Roland PE. 1996. Two different areas within the primary motor cortex of man. Nature. 382:805–807.
He SQ, Dum RP, Strick PL. 1993. Topographic organization of corticospinal projections from the frontal lobe: motor areas on the lateral surface of the hemisphere. J Neurosci. 133:952–980.
Hendry SH, Jones EG. 1981. Sizes and distributions of intrinsic neurons incorporating tritiated GABA in monkey sensory-motor cortex. J Neurosci. 1:390–408.
Hoshi E, Tanji J. 2007. Distinctions between dorsal and ventral premotor areas: anatomical connectivity and functional properties. Curr Opin Neurobiol. 17:234–242.
Isa T, Kinoshita M, Nishimura Y. 2013. Role of direct vs. indirect pathways from the motor cortex to spinal motoneurons in the control of hand dexterity. Front Neurol. 4:191.
Jeannerod M, Arbib MA, Rizzolatti G, Sakata H. 1995. Grasping objects: the cortical mechanisms of visuomotor transformation. Trends Neurosci. 18:314–320.
Johnson PB, Ferraina S, Bianchi L, Caminiti R. 1996. Cortical networks for visual reaching: physiological and anatomical organization of frontal and parietal arm regions. Cereb Cortex. 6(2):102–119.
Kantak SS, Stinear JW, Buch ER, Cohen LG. 2012. Rewiring the brain: potential role of the premotor cortex in motor control, learning, and recovery of function following brain injury. Neurorehabil Neural Repair. 26:282–292.
Keller A, Asanuma H. 1993. Synaptic relationships involving local axon collaterals of pyramidal neurons in the cat motor cortex. J Comp Neurol. 336:229–242.
Kraskov A, Philipp R, Waldert S, Vigneswaran G, Quallo MM, Lemon RN. 2014. Corticospinal mirror neurons. Philos Trans R Soc B. 369:20130174.
Lemon RN. 1988. The output map of the primate motor cortex. Trends Neurosci. 11:501–506.
Lemon RN. 2008. Descending pathways in motor control. Annu Rev Neurosci. 31:195–218.
Lemon RN. 2010. What drives corticospinal output? Biol Rep. 2:51.
Livingston SC, Goodkin HP, Ingersoll CD. 2010. The influence of gender, hand dominance, and upper extremity length on motor evoked potentials. J Clin Monit Comput. 24:427–436.
Maier M, Armand J, Kirkwood PA, Yang HW, Davis JN, Lemon RN. 2002. Differences in the corticospinal projection from primary motor cortex and supplementary motor area to macaque upper limb motoneurons: an anatomical and electrophysiological study. Cereb Cortex. 12:281–296.
Maier MA, Kirkwood PA, Brochier T, Lemon RN. 2013. Responses of single corticospinal neurons to intracortical stimulation of primary motor and premotor cortex in the anesthetized macaque monkey. J Neurophysiol. 109:2982–2998.
Maranesi M, Roda F, Bonini L, Rozzi S, Ferrari PF, Fogassi L, Coude G. 2012. Anatomo-functional organization of the ventral primary motor and premotor cortex in the macaque monkey. Eur J Neurosci. 36:3376–3387.
Markram H, Wang Y, Tsodyks M. 1998. Differential signaling via the same axon of neocortical pyramidal neurons. Proc Natl Acad Sci. 95:5323–5328.
Morecraft RJ, Ge J, Stilwell-Morecraft K, McNeal D, Pizzimenti MA, Darling WG. 2013. Terminal distribution of the corticospinal projection from the hand/arm region of the primary motor cortex to the cervical enlargement in rhesus monkey. J Comp Neurol. 521:4205–4235.
Mink JW. 1996. The basal ganglia: focused selection and inhibition of competing motor programs. Prog Neurobiol. 50:381–425.
Nelissen K, Luppino G, Vanduffel W, Rizzolatti G, Orban G. 2005. Observing others: Multiple action representation in the frontal lobe. Science. 310:332–336.
Orban G. 2002. Functional MRI in the awake monkey: the missing link. J Cogn Neurosci. 14:965–969.
Patton HD, Amassian V. 1954. Single and multiple-unit analysis of cortical stage of pyramidal tract activation. J Neurophysiol. 17:345–363.
Penfield W, Boldrey E. 1937. Somatic motor and sensory representation in the cerebral cortex of man as studied by electrical stimulation. Brain. 9:389–443.
Porter R, Lemon RN. 1993. Corticospinal function and voluntary movement. Oxford: Oxford University Press.
Prabhu G, Shimazu H, Cerri G, Brochier T, Spinks RL, Maier MA, Lemon RN. 2009. Modulation of primary motor cortex outputs from ventral premotor cortex during visually guided grasp in the macaque monkey. J Neurophysiol. 587:1057–1069.
Quiñones-Hinojosa A, Ojemann SG, Sanai N, Dillon WP, Berger MS. 2003. Preoperative correlation of intraoperative cortical mapping with magnetic resonance imaging landmarks to predict localization of the Broca area. J Neurosurg. 99:311–318.
Raos V, Franchi G, Gallese V, Fogassi L. 2003. Somatotopic organization of the lateral part of area F2 (dorsal premotor cortex) of the macaque monkey. J Neurophysiol. 89: 1503–1518.
Raos V, Umiltà MA, Gallese V, Fogassi L. 2004. Functional properties of grasping-related neurons in the dorsal premotor area F2 of macaque monkey. J Neurophysiol. 92:1990–2002.
Raos V, Umilta MA, Murata A, Fogassi L, Gallese V. 2006. Functional properties of grasping-related neurons in the ventral premotor area f5 of the macaque monkey. J Neurophysiol. 95:709–729.
Rathelot JA, Strick PL. 2006. Muscle representation in the macaque motor cortex: an anatomical perspective. Proc Natl Acad Sci. 103:8257–8262.
Rathelot JA, Strick PL. 2009. Subdivisions of primary motor cortex based on cortico-motoneuronal cells. Proc Natl Acad Sci. 106:918–923.
Rizzolatti G, Cattaneo L, Fabbri-Destro M, Rozzi S. 2014. Cortical mechanisms underlying the organization of goal-directed actions and mirror neuron-based action understanding. Physiol Rev. 94:655–706.
Sanes JN, Donoghue JP, Thangaraj V, Edelman RR, Warach S. 1995. Shared neural substrates controlling hand movements in human motor cortex. Science. 268:1775–1777.
Schieber MH. 1991. Individuated finger movements of rhesus monkeys: a means of quantifying the independence of the digits. J Neurophysiol. 65:1381–1391.

Schieber MH. 2001. Constraints on somatotopic organization in the primary motor cortex. J Neurophysiol. 86:2125–2143.

Schmidlin E, Brochier T, Maier MA, Kirkwood PA, Lemon RN. 2008. Pronounced reduction of digit motor responses evoked from macaque ventral premotor cortex after reversible inactivation of the primary motor cortex hand area. J Neurosci. 28:5772–5783.

Schulz R, Park CH, Boudrias MH, Gerloff C, Hummel FC, Ward NS. 2012. Assessing the integrity of corticospinal pathways from primary and secondary cortical motor areas after stroke. Stroke. 43:2248–225.

Schulz R, Braass H, Liuzzi G, Hoerniss V, Lechner P, Gerloff C, Hummel FC. 2014. White matter integrity of premotor–motor connections is associated with motor output in chronic stroke patients. NeuroImage Clin. 7:82–86.

Shattuck DW, Leahy RM. 2002. BrainSuite: an automated cortical surface identification tool. Med Image Anal. 6: 129–142.

Shimazu H, Maier MA, Cerri G, Kirkwood PA, Lemon RN. 2004. Macaque ventral premotor cortex exerts powerful facilitation of motor cortex outputs to upper limb motoneurons. J Neurosci. 24:1200–1211.

Silberberg G, Markram H. 2007. Disynaptic inhibition between neocortical pyramidal cells mediated by Martinotti cells. Neuron. 53:735–746.

Simonyan K, Jurgens U. 2003. Efferent subcortical projections of the laryngeal motor cortex in the rhesus monkey. Brain Res. 974:43–59.

Simonyan K, Jürgens U. 2005. Afferent cortical connections of the motor cortical larynx area in the rhesus monkey. Neuroscience. 130:133–149.

Sohn YH, Hallett M. 2004. Surround inhibition in human motor system. Exp Brain Res. 158:397–404.

Stoney SD, Thompson WD, Asanuma H. 1968. Excitation of pyramidal tract cells by intracortical microstimulation: effective extent of stimulating current. J Neurophysiol. 31:659–669.

Tadel F, Baillet S, Mosher JC, Pantazis D, Leahy RM. 2011. Brainstorm: a user-friendly application for MEG/EEG analysis. Comput Intell Neurosci. 2011:879716.

Tomasch J. 1969. The numerical capacity of the pontine cell and fibre systems. J Anat. 104:187.

Tokuno H, Takada M, Nambu A, Inase M. 1997. Reevaluation of ipsilateral corticocortical inputs to the orofacial region of the primary motor cortex in the macaque monkey. J Comp Neurol. 389:34–48.

Umiltà MA, Brochier T, Spinks RL, Lemon RN. 2007. Simultaneous recording of macaque premotor and primary motor cortex neuronal populations reveals different functional contributions to visuomotor grasp. J Neurophysiol. 98:488–501.

Umiltà MA, Escola L, Intskirveli I, Grammont F, Rochat M, Caruana F, Jezzini A, Gallese V, Rizzolatti G. 2008. When pliers become fingers in the monkey motor system. Proc Natl Acad Sci USA. 105:2209–2213.

Verstynen T, Jarbo E, Pathak S, Schneider W. 2011. In Vivo mapping of microstructural somatotopies in the human corticospinal pathways. J Neurophysiol. 105:336–346.

Vigneswaran G, Kraskov A, Lemon RN. 2011. Large identified pyramidal cells in macaque motor and premotor cortex exhibit “thin spikes”: implications for cell type classification. J Neurosci. 31:14235–14242.

Wise SP, Boussaud D, Johnson PB, Caminiti R. 1997. Premotor and parietal cortex: corticocortical connectivity and combinatorial computation. Annu Rev Neurosci. 20:25–42.

Ziemann U, Rothwell JC, Ridding MC. 1996. Interaction between intracortical inhibition and facilitation in human motor cortex. J Physiol. 496:873–881.